Changes in Intra-axonal Calcium Distribution Following Nerve Crush

MARINA MATA,* JULIE STAPLE, and DAVID J. FINK

Neurology Research Laboratory, University of Michigan and VA Medical Center, Ann Arbor, MI 48105

Received April 24, 1986

SUMMARY

We used the oxalate-pyroantimonate method to demonstrate the ultrastructural distribution of calcium within rat sciatic nerve 4 h after a crush injury. In normal nerve there are discrete gradients of axoplasmic calcium precipitate with the amount of precipitate decreasing in the axoplasm beneath the Schmidt Lantermann clefts and in the paranodal regions at the node of Ranvier. Near the crush site a marked increase in endoneurial and intra-axonal calcium precipitate correlated with morphologic evidence of axonal degeneration. More distant from the crush site, both in the distal segment destined to degenerate and in the proximal segment destined to regenerate, the most prominent finding was a loss of the normal gradient of precipitate beneath the Schmidt Lantermann clefts. The calcium influx at the crush site corresponds to the known role of calcium in triggering degeneration. The alterations in the distal axon may be an early stage leading to degeneration. Alteration in calcium distribution in the proximal nerve stump may play a role in the regulation of the response to injury.

INTRODUCTION

Following the crush of a peripheral nerve the fates of the two segments of the axon are widely divergent. The segment distal to the injury, deprived of its connection to the cell body undergoes Wallerian degeneration. Irregular swelling of the axon is followed by granular disintegration of the axoplasmic matrix and progressive degenerative changes in organelles leading to fragmentation of the axoplasm (Sunderland, 1978). Identical changes in neurofilament structure and the production of breakdown products can be reproduced in excised nerve, where the phenomenon has been shown to be calcium dependent, mediated by the activation of an endogenous protease (Schlaepfer and Micko, 1978, 1979; Schlaepfer et al., 1985).

The axon proximal to the transection, still in continuity with the cell body, appears morphologically unchanged except at the terminal stump where a process of axonal sprouting is followed by axonal elongation into the distal endoneurial sheaths (Friede and Bischausen, 1980). If the normal axon is conceived of as the study state of a system in rapid flux, with the

* To whom all correspondence should be addressed at: Neurology Service (127), 2215 Fuller Road, Ann Arbor, MI 48105.

Journal of Neurobiology, Vol. 17, No. 5, pp. 449–467 (1986)
 CCC 0022-3034/86/050449-19$04.00

introduction of proteins into the axon by rapid and slow axonal transport balanced by their release, turnover, or recycling to the cell body, the regenerating axon is more remarkable for its similarity to the normal axon than for major differences. This suggests that the process of regeneration must depend to some extent upon local regulation within the axon controlling sprouting and elongation.

In order to delineate the role of calcium influx in the production of Wallerian degeneration in the distal axon, and to explore the possible role of alterations in calcium flux in the local regulation of the proximal axonal response to injury, we undertook this study of the ultrastructural localization of calcium in nerve following injury using an oxalate-pyroantimonate technique (Borgers et al., 1977). Oxalate is used to specifically chelate calcium during primary fixation while other cations are washed out, followed by fixation with pyroantimonate producing electron dense calcium pyroantimonate precipitates. We have used this method to define the distribution of calcium within normal rat sciatic nerve (Mata et al., submitted). In this study we describe alterations in that distribution 4 h after a nerve crush in the segments both proximal and distal to the crush.

METHODS

Male Sprague Dawley rats weighing 250–300 g were anesthetized with chloral hydrate, the right sciatic nerve exposed in the gluteal region and crushed for 1 min with a jeweler's forceps. At 4 h after crush the animal was reanesthetized and perfused through the heart with 90mM potassium oxalate in 1.9% sucrose, adjusted to pH 7.4 with KOH, at 37°C for 2 min, followed by 3% glutaraldehyde, 0.5% paraformaldehyde, 90mM potassium oxalate, 1.9% sucrose adjusted to pH 7.4 with KOH for approximately 1 h at a constant perfusion rate. At the conclusion of the perfusion, the sciatic nerve, the L4, L5, and L6 dorsal root ganglia with the corresponding dorsal and ventral roots and gastrocnemius muscle were removed and maintained in the same fixative solution at 4°C for 2 h. They were then rinsed in 90mM potassium oxalate in 1.9% sucrose, pH 7.4, postfixed in 1% osmium tetraoxide, 2% potassium pyroantimonate for 2 h, rinsed in water adjusted to pH 10 with KOH for 15 min, dehydrated in alcohol, and embedded in a Polybed-Araldite mixture. Semithin and ultrathin sections were prepared on an LKB Nova Ultratome, picked up on uncoated nickel grids, and examined without post-staining in a JEOL-100S electron microscope. Occasionally specimens were stained with uranyl acetate to improve contrast. All such stained specimens are noted in the figure legends.

The nerve segments were labeled according to their proximity to the crush site, and whether they were proximal to or distal from the crush. The contralateral nerve and dorsal root ganglia served as control.

In order to demonstrate the specificity of the reaction, several controls were performed. In the first control 2% potassium pyroantimonate was deleted from the postfixation and 90mM potassium oxalate used in its place. In the second control the ultrathin sections supported on the grids were washed in 10mM EGTA pH8 at 60°C for 1 h. Parallel grids washed in water adjusted to pH8 with KOH at 60°C for 1 h served as internal controls. X-ray microanalysis of the precipitate in the axoplasm was performed on 100–200 nm unstained sections on nickel grids with a JEOL-100CX electron micro-

scope equipped with a KEVEX 3212 SMS-V energy dispersive spectrometer (accelerating voltage 100–200 kV, tilt angle of the preparation 35° and collection time of spectral lines 180–2000 s real time). The K_{alpha} and K_{beta} calcium peaks and the L_{alpha} and L_{beta} antimonate peaks occur in the same region, respectively, and the peaks overlap. The K_{beta} peak of potassium also overlaps with the K_{alpha} peak of calcium. To demonstrate the presence of calcium, the calcium, potassium, and antimonate spectrums obtained were deconvoluted using the "multiple least square fit" method (Schamber et al., 1977) as adapted to a Nuclear Data 6620 computer.

RESULTS

The nerves from 3 animals at 4 h after crush were analyzed in detail. Contralateral to the crush the calcium distribution was identical to that seen in unoperated control animals. We have recently described that distribution in detail (Mata et al., submitted). In brief, a fine reticular pattern of calcium pyroantimonate precipitate was seen throughout the axoplasm in a predominently linear distribution more prominent in the subaxolemmal region and in the neurofilament domains. Calcium precipitate was also seen in the smooth endoplasmic reticulum and less prominantly within the mitochondria [Fig. 1(A)]. The energy spectrum obtained by X-ray microanalysis of similar areas of axoplasm containing the precipitate is seen in Fig. 1(C), which shows the overlapping K_{alpha} and K_{beta} peaks of calcium with the L_{alpha} and L_{beta} peaks of antimony. The amount of calcium in the spectrum was determined by deconvolution using the "multiple least square fit" method and it ranged from 278 to 403 counts above background, corresponding to 14–17% of the total counts in the K_{alpha} and K_{beta} regions of calcium. This was a statistically significant amount according to the method of Roomans (1980).

Consecutive serial sections washed with EGTA as described in the methods showed loss of precipitate [Fig. 1(B)]. X-ray microanalysis of similar areas of axoplasm treated with EGTA showed the absence of the combined calcium antimonate peak [Fig. 1(D)], while parallel sections rinsed in water adjusted to pH 8 with KOH for a similar length of time did not lose the precipitate. Tissue treated with 90 mM potassium oxalate instead of potassium pyroantimonate during the postfixation contained no precipitate.

In unmyelinated axons the amount of precipitate appeared homogeneous throughout the length of the axon, while in myelinated fibers there was a marked decrease in the amount of precipitate in the axoplasm beneath the Schmidt Lantermann clefts in 75% of the clefts in normal nerve [Fig. 2(A)], and in the axoplasm in the paranodal regions at the node of Ranvier [Fig. 3(A)]. Beneath the node itself the amount of precipitate was similar to that seen in internodal regions. Dense precipitate was found in the Schmidt Lantermann clefts themselves and in the paranodal loops of myelin.

In the crush nerve the segments immediately adjacent to the crush site showed obvious evidence of degeneration. There was clumping of the axoplasmic matrix, accumulation of vesicular organelles, swelling of the mitochondria, and fragmentation of the axoplasm with retraction from the myelin sheath. Vesicular degeneration of the myelin was seen most often at the Schmidt Lantermann clefts. The changes were more severe in some fibers than in others. Accompanying the morphologic changes there was

Fig. 1. (A) Calcium pyroantimonate distribution in the axoplasm of a myelinated fiber. The precipitate forms a linear longitudinal pattern in the axoplasm and is also seen in the smooth endoplasmic reticulum (arrowhead) and mitochondria (arrow). ×27,500, stained with uranyl acetate, bar = 1 micron. (B) Immediate serial section of the same fiber treated with 10mM EGTA, pH 8, for 1 h. Note the absence of precipitate. ×27,500, stained with uranyl acetate, bar = 1 micron.(C) X-ray microanalysis of the axoplasm. The overlapping spectrum of the K_{alpha} and K_{beta} peaks of calcium and the L_{alpha} and L_{beta} peaks of antimonate are shown. The K_{alpha} of calcium occurs at 3.69 KeV. The total counts of calcium in the peak was determined by deconvolution as described in the text. The peaks of osmium (1.91 KeV) and chloride (2.62 KeV) are also seen. (D) X-ray microanalysis of the axoplasm of a myelinated fiber treated with EGTA. The absence of the calcium antimonate peaks correlate with the absence of precipitate as seen in (B).

increased amount of precipitate in axoplasm and in swollen organelles, particularly mitochondria both in fibers which were degenerating, as well as in fibers with less obvious pathologic changes (Fig. 4). In the 4 mm segment just proximal to the crush site, similar morphologic evidence of degeneration and accumulation of calcium precipitate were found (Fig. 5). The nodes of Ranvier near the crush site showed widening of the nodal gap and retraction of the paranodal myelin with accumulation of vesicular or-

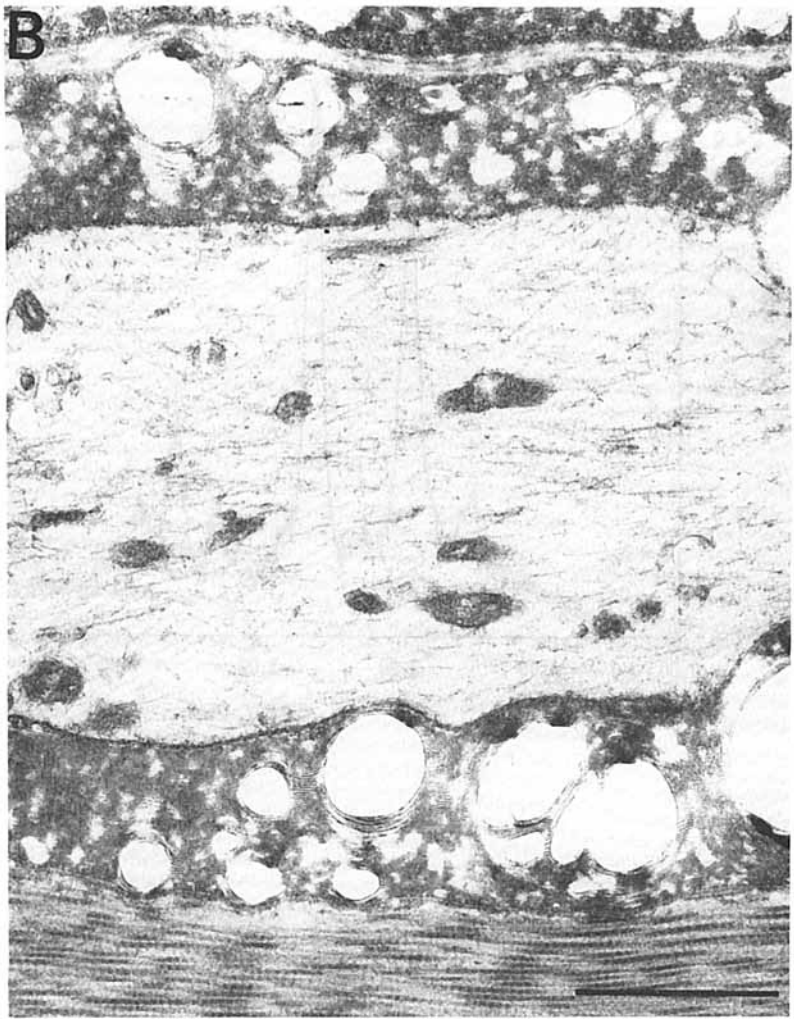

Fig. 1. (*Continued from previous page.*)

ganelles and lamellar bodies, accompanied by marked accumulation of calcium and obliteration of the normal gradients at the paranodal regions (Fig. 6). Both proximal and distal to the crush site the changes were most pronounced nearest to the crush.

Four to twelve millimeters distal from the crush site most fibers appear to become progressively more normal ultrastructurally. Many of the fibers appeared to have an increased amount of precipitate. Even in those fibers in which the amount of precipitate appeared normal in the axoplasm, the mitochondria and smooth endoplasmic reticulum contained increased amounts of precipitate. Most strikingly, the normal gradients of precipitate in the axoplasm at the Schmidt Lantermann clefts was lost. In the distal segment gradients were seen in only 26% of the clefts (Table 1). Calcium precipitate at the nodes of Ranvier, however, appeared still to have a normal distribution [Fig. 3(B)].

Similarly, in the proximal nerve stump, 4–12 mm proximal to the crush site virtually all the fibers appeared ultrastructurally normal. While a few

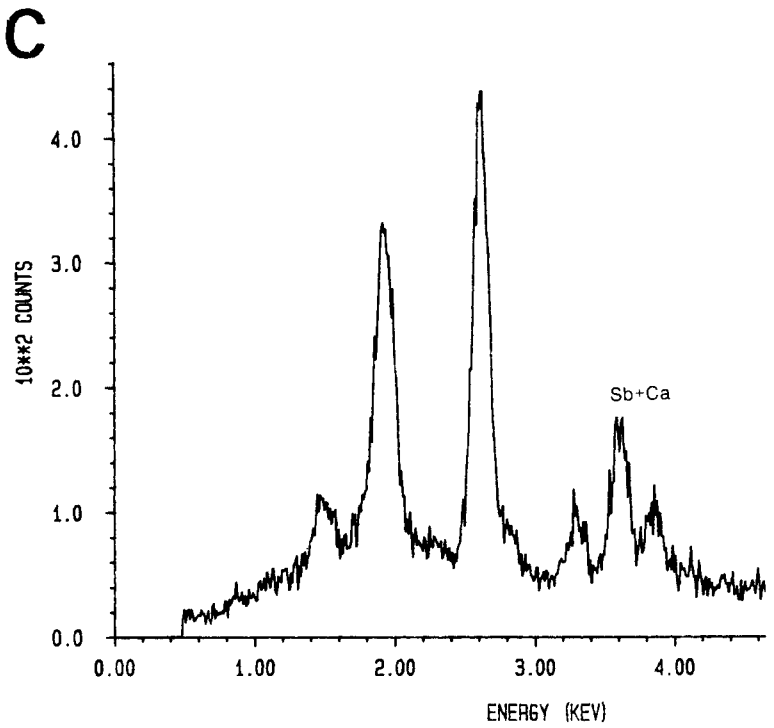

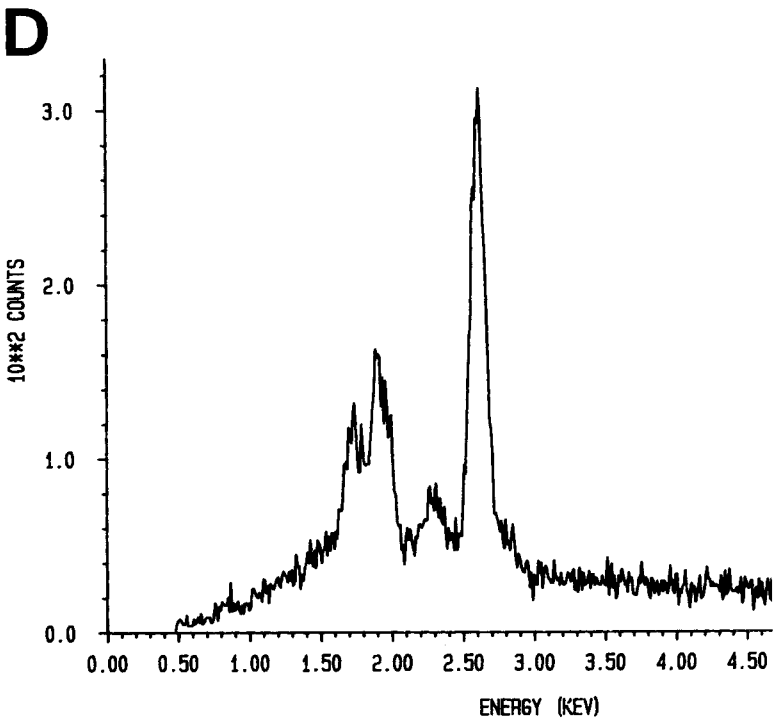

Fig. 1. (*Continued from previous page.*)

fibers contained excess precipitate, more fibers had mitochondria containing a large amount of precipitate. The characteristic distribution of axoplasmic precipitate at the node of Ranvier and the longitudinal orientation more prominent in the regions of neurofilaments were still present. However, like the distal segment, there was obvious loss of the normal gradient of precipitate in the axoplasm beneath the Schmidt Lantermann clefts [Fig. 2(B)]. Only 29% of the proximal clefts had a gradient of precipitate (Table 1).

Like the axonal changes, the endoneurium was more markedly altered nearest to the crush site. In the segments immediately adjacent to the crush the endoneurial space was enlarged and often contained large amounts of calcium precipitate. Endoneurial blood vessels in this region contained dense calcium precipitate in the nuclei, cytosol and mitochondria of the endothelial cells and pericytes. Segments taken 10–12 mm from the crush site had normal appearing endoneurium with precipitate that appeared identical to the control.

DISCUSSION

We have used the oxalate pyroantimonate method to discern the ultrastructural localization of mobilizable calcium in rat sciatic nerve at 4 h after a crush injury to the nerve. Using this method we have found that there are alterations in the distribution of calcium both in the nerve distal to the crush which is destined to undergo Wallerian degeneration as well as in the nerve proximal to the crush which is destined to regenerate.

The Oxalate-Pyroantimonate Method. In order to define the ultrastructural localization of calcium in noncalcified tissues, a number of methods have been developed during the past decade. The addition of calcium during fixation for electron microscopy creates electron dense precipitate, apparently at specific calcium binding sites in the cell (Oschman and Wall, 1972; Hillman and Llinas, 1974). Other investigators have used oxalate or pyroantimonate after calcium loading in vitro to demonstrate sites of binding or sequestration of exogenous calcium (Henkart et al., 1978; Chan et al., 1984). Pyroantimonate precipitates endogenous calcium, and by adding pyroantimonate to the primary fixative others have defined precipitates bound to membrane as well as distribute through the cytoplasm in a number of cell types (Duce and Keen, 1978).

We have used a modification of the basic method described by Borgers et al. (1977) in which oxalate is used to chelate calcium before precipitation with pyroantimonate. In any ultrastructural method of this type it is critical to demonstrate that the precipitates found reflect calcium specifically. We have used two controls. Deleting the pyroantimonate resulted in absence of precipitate, demonstrating the pyroantimonate component of the precipitate. Washing with EGTA removed the precipitate, demonstrating the calcium component. In addition, X-ray microanalysis of the axoplasm revealed that the precipitate contained calcium, accounting for about 15% of the counts in the combined spectrum.

Unlike some other ultrastructural methods, this oxalate-pyroantimonate method produces a precipitate which is not bound to membranes. The pre-

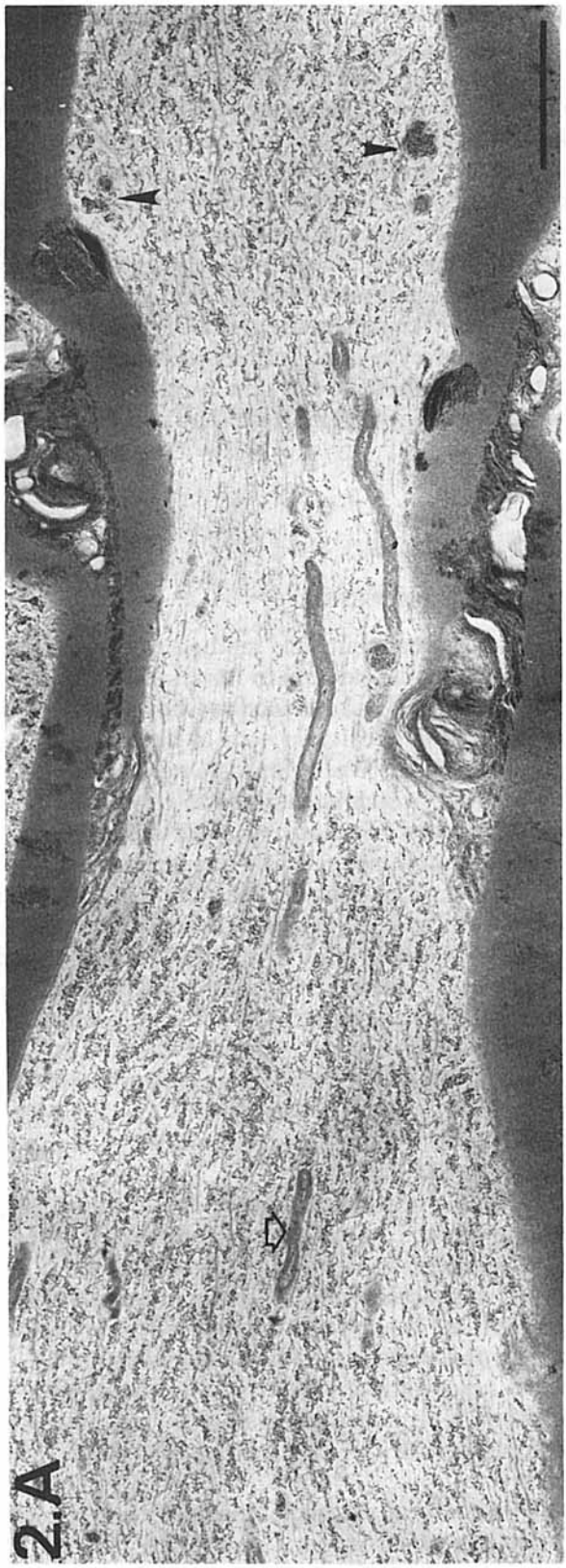

Fig. 2. (A) Gradient of calcium precipitate seen in the axoplasm of a normal nerve fiber beneath of Schmidt Lantermann cleft. Precipitate is also seen in the tubulovesicular profiles of smooth endoplasmic reticulum (arrowhead) and mitochondria (arrow). Stained with uranyl acetate, bar = 1 micron. (B) A Schmidt Lantermann cleft 8–12 mm proximal to the crush site at 4 h after nerve crush. Although the fiber appears structurally normal and is in continuity with the cell body, there is a loss of the normal gradient in the distribution of calcium pyroantimonate precipitate at the cleft (compare with (A). ×15,000, stained with uranyl acetate, bar = 1 micron.

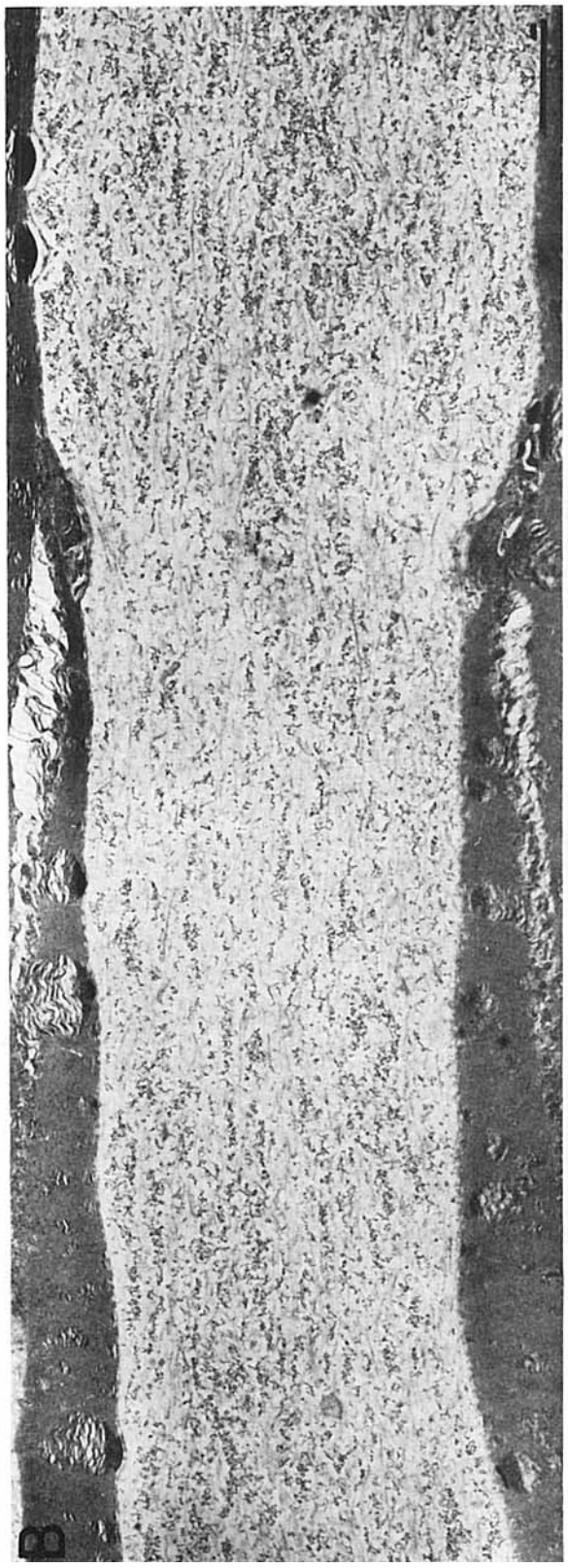

Fig. 2. *(Continued from previous page.)*

Fig. 3. (A) Gradients of calcium precipitate seen in the axoplasm in the paranodal regions at the node of Ranvier of a normal nerve fiber. ×22,000, stained with uranyl acetate, bar = 1 micron. (B) A node of Ranvier, 8–12 mm distal from the crush site at 4 h after nerve crush. The node has a distribution of calcium precipitate similar to a normal node, although there is an increased amount of precipitate within mitochondria (arrow) and smooth endoplasmic reticulum (arrowhead). ×20,000, stained with uranyl acetate, bar = 1 micron.

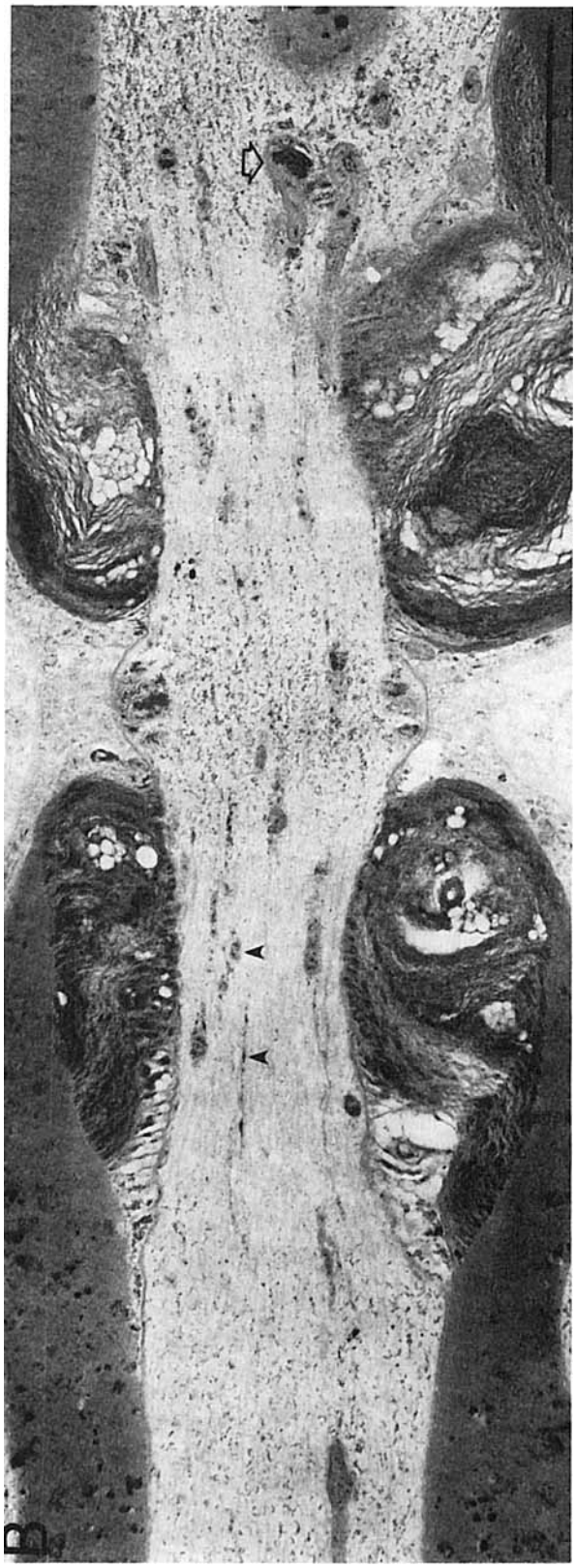

Fig. 3. *(Continued from previous page.)*

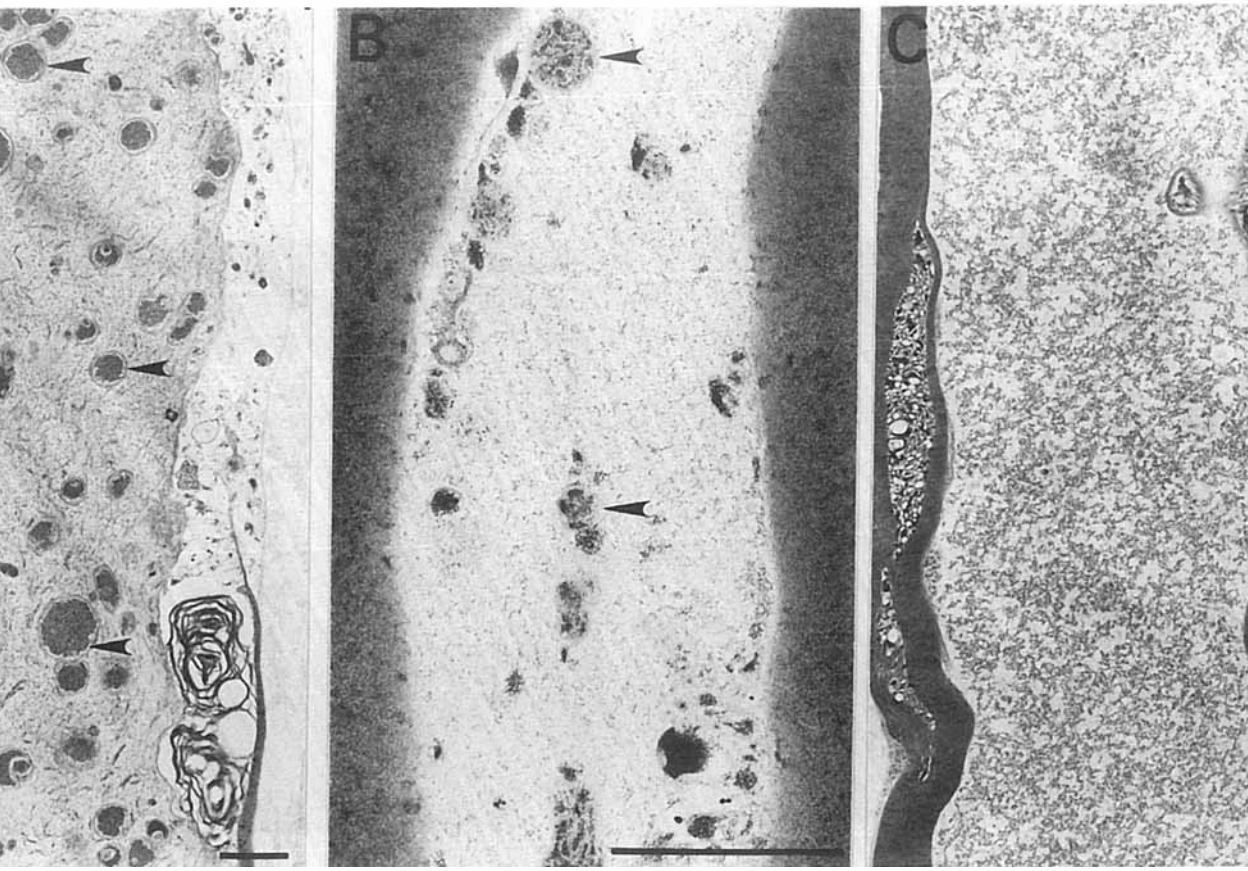

yelinated axons in the first 4 mm distal to a crush, 4 h after nerve crush. There is a marked accumulation of calcium prec
d swollen, distorted organelles (arrowhead). Note the vesicular disruption of the myelin in (C). (A) ×97,500; (B) ×31,200; (C
uranyl acetate, bar = 1 micron.

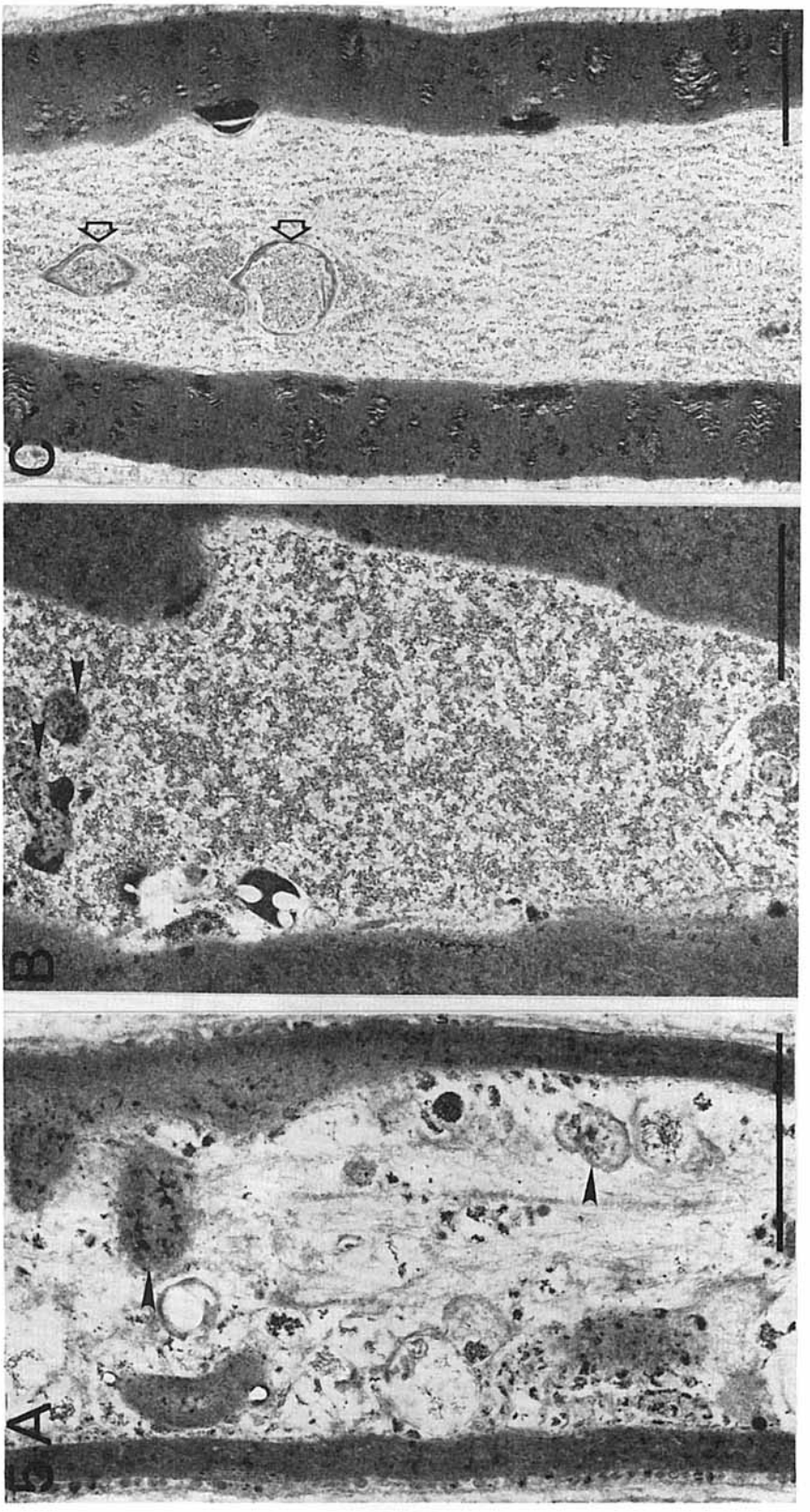

Fig. 5. Myelinated axons in the first 4 mm segment just proximal to the crush site, 4 h after nerve crush. There is a marked variability in the degree of morphologic disruption in different fibers. There is increased calcium precipitate in the axoplasm and in organelles (arrowhead), even in the best preserved axons as seen in the mitochondria in (C) (arrow). (A) ×20,000; (B) × 22,250; (C) × 16,500, stained with uranyl acetate, bar = 1 micron.

Fig. 6. A node of Ranvier just proximal to the crush site at 4 h after nerve crush. There is marked disruption of the axoplasm and widening of the nodal gap with retraction of the paranodal myelin. There is marked accumulation of calcium precipitate in the axoplasm and loss of the gradients in precipitate distribution normally seen in the paranodal region. Similar changes were found immediately distal to the crush site. ×11,100, stained with uranyl acetate, bar = 1 micron.

TABLE 1
Distribution of Calcium Precipitate in the Axoplasm Beneath the Schmidt Lanterman Clefts[a]

Site	Number of Clefts	Number with Gradient
Control	106	75
Proximal (4–12 mm)	128	38 $P < 0.0001$
Distal (4–12 mm)	118	31 $P < 0.0001$

[a] The sections of nerve proximal to the crush, distal to the crush, and the control side were analyzed for the presence or absence of a gradient. A total of 352 clefts from three crush and three contralateral control nerves were analyzed. The significance of the differences was determined using a Chi square test.

cipitate appears free in the axoplasm, and when it is associated with membranous organelles like smooth endoplasmic reticulum or mitrochondria is found within those structures. Borgers has suggested, and we agree, that the oxalate pyroantimonate method appears to define the distribution of a particular mobilizable pool of calcium (Borgers et al., 1984). Calcium is present in nerve cells in millimolar amounts, but as a result of sequestration in organelles, complexing to anions, and binding to various sites within the cell, the free cytosolic calcium is generally accepted to be in the range of 10^{-7}M (Campbell, 1983). Because of the marked differences in distribution of precipitate between the various ultrastructural methods we think it unlikely that any of the methods reflects the total calcium in the cell, but rather that each shows the distribution of a particular pool. For instance, we find that the amount of precipitate between the cristae within normal mitochondria is in general less than that found within the axoplasm or tubulovesicular profiles of smooth endoplasmic reticulum. This suggests that the chelatable pool of calcium in the mitochondria is less than that in the axoplasm or endoplasmic reticulum, but does not address the issue of how much total calcium each organelle sequesters in the normal nerve.

We have previously found that the calcium precipitate within the axoplasm is heterogeneously distributed (Mata et al., submitted). In normal nerve there are reproducible gradients of precipitate within the axoplasm. The amount of precipitate decreases in the axoplasm beneath the Schmidt Lantermann clefts and in the axoplasm in the paranodal regions at the node of Ranvier. We have speculated that this distribution may reflect restricted sites of influx and extrusion of calcium in normal nerve, with calcium entering the axoplasm principally at the node of Ranvier and being pumped out at the paranodal regions and through the axolemma at the Schmidt Lantermann clefts. A second possibility is that this heterogeneous distribution of precipitates reflects the heterogeneous distribution of calcium binding proteins within the axoplasmic matrix. The reproducible distribution of precipitate within the axoplasm suggests that the heterogeneity observed in fact reflects the distribution of this particular pool of calcium within the axoplasm. In addition, the finding in the current study that experimental manipulation of the nerve prior to perfusion-fixation alters this distribution of calcium precipitate in a specific manner is strong evidence that the heterogeneous distribution is biologically significant.

Calcium in the Distal Nerve Segment after Crush. The distal nerve segment after crush is destined to undergo Wallerian degeneration. Some

aspects of this process appear to progress from the crush site distally in the nerve, faster in small diameter fibers than in large diameter fibers (Williams and Hall, 1971; Lubinska, 1977), while other changes may occur rapidly and simultaneously throughout the distal stump (Malbouisson et al., 1984, 1985).

At 4 h after crush we have found that near the crush site, where evidence of degeneration is prominent, there is a marked increase in calcium precipitate both in the endoneurial space and within the degenerating axons, within the axoplasm and within swollen distorted organelles. This is in agreement with the findings of Wade et al. (1980) that degenerating myelinated axons in rat brain show increased calcium antimonate within the axoplasm and intra-axonal organelles. In experimental spinal cord trauma the amount of calcium measured by atomic absorption spectroscopy increases significantly at the site of a crush (Happel et al., 1981). Extracellular calcium ionic activity measured with a calcium sensitive microelectrode shows a fall compatible with a shift from extracellular to intracellular calcium beginning within minutes after injury (Young et al., 1982). Late after spinal cord trauma, intra-axoplasmic deposits of hydroxyapatite crystals may be seen (Balentine and Spector, 1977; Balentine, 1983).

Indirect evidence strongly implicates calcium influx in triggering Wallerian degeneration. The same changes of granular disintegration of neurofilaments can be reproduced in excised nerves where it has been demonstrated to be a calcium dependent phenomenon (Schlaepfer and Micko, 1978, 1979). A calcium activated protease has been isolated from brain and spinal cord and identified in peripheral nerve (Kamakura et al., 1981; Malik et al., 1983; Zimmerman and Schlaepfer, 1982). Homologous patterns of neurofilament fragmentation in transected sciatic nerve fibers and in the calcium activated proteolysis of isolated neurofilaments by isolated protease suggest that the protease is activated in Wallerian degeneration (Schlaepfer et al., 1985). A calcium activated myelinase has also been presumptively identified in spinal cord by its calcium stimulated activity in vitro.

The increased amount of precipitate we find in the segments of nerve where degeneration is occurring supports this interpretation of the role of calcium. The mitochondria in these segments show a marked accumulation of calcium precipitate, presumably due to mitochondrial sequestration of the entering calcium. More distally, where regeneration is not yet apparent, we find some increase in mitochondrial and axoplasmic precipitate in many fibers and a consistent loss of the gradients normally found beneath Schmidt Lantermann clefts. We anticipate that the progressive proximal to distal changes of Wallerian degeneration will be preceded by loss of the gradient and detectable accumulation of calcium precipitate within the nerve fibers and organelles.

Calcium in the Proximal Nerve Stump after Crush. Immediately proximal to the crush site damaged degenerating fibers contain large amounts of calcium precipitate, similar to the distal nerve stump. This calcium influx should trigger the calcium activated protease implicated in degeneration as described above, and is likely to be responsible for the ultrastructural changes at the crush site. An unexpected finding was that in the nerve segments more distant from the crush site in the proximal stump, there was loss of gradients in the calcium distribution beneath the Schmidt Lantermann clefts similar to that seen in the distal segment.

There is no previous data to suggest that alterations in calcium occur in the nerve proximal to a crush. Ultrastructurally these axons appear normal, and they are in large part destined to regenerate successfully through the crush site. It is intriguing to speculate that alterations in the calcium distribution in the proximal stump might play a role in regulating the response of the axon to injury. It has recently been demonstrated that influx of calcium at the cut end of the cockroach giant axon triggers membrane resealing by activating phospholipase A_2 (Yawo and Kuno, 1983, 1985). Calcium has previously been demonstrated to play a role in both axonal transport of macromolecules (Chan et al., 1980), as well as in regulating the state of polymerization of microtubules (Schliwa, 1976), and alterations in either of these might be involved in the conversion from steady state to regenerating axon.

There are several possible explanations for the alteration of distribution of calcium within the nerve. Following a crush the blood nerve barrier is disrupted at the crush site (Olsson, 1966), and becomes more permeable both proximal and distal to the crush, which should cause increased endoneurial calcium. In addition, there is an influx of calcium into axons at the injury site (Borgens et al., 1980), as well as transient electrical discharges related to injury (Kirk, 1974) which might cause calcium influx. While both of these may occur, they do not explain the preservation of normal gradients in the paranodal regions while there is loss of the gradients at the Schmidt Lantermann clefts.

We have suggested previously that the areas of decreased calcium precipitate beneath the Schmidt Lantermann clefts may represent a site of calcium extrusion in normal nerve. If this were true, a reduction in the rate of calcium pumping would cause the loss of the normal gradient within the axoplasm and trigger the calcium associated changes in the proximal stump leading to regeneration.

In any case these experiments clearly demonstrate that the heterogeneous distribution of calcium which we have reported in normal axons is specifically altered at 4 h after a nerve crush. These results appear to confirm the previously reported role for calcium influx in triggering Wallerian degeneration, and suggest that alterations in calcium distribution may help to regulate the axonal response to injury.

This work was supported by VA Merit Review Grants to Dr. Mata and to Dr. Fink. The authors would like to express appreciation to Dr. W. C. Bigelow and H. Honke from the Department of Materials and Metallurgical Engineering at the University of Michigan for their assistance in the microanalysis and deconvolution of the spectra, and to C. Johnson and C. White for excellent secretarial assistance. Protions of this work were presented in abstract form at the meeting of the American Academy of Neurology in Dallas, Texas in April 1985.

REFERENCES

BALENTINE, J. E., and SPECTOR, M. (1977). Calcification of axons in experimental spinal cord trauma. *Ann. Neurol.* **2:** 520–523.

BALENTINE, J. D. (1983). Calcium toxicity as a factor in spinal cord injury. *Surv. Synth. Path. Res.* **2:** 184–193.

BORGENS, R. B., JAFFE, L. F., and COHEN, M. J. (1980). Large and persistent electrical currents enter the transected lamprey spinal cord. *Proc. Natl. Acad. Sci.* **77:** 1209–1213.

BORGERS, M., DE BRABANDER, M., VAN REEMPTS, J., AWOUTERS, F., and JACOB, W. A. (1977). Intranuclear microtubules in lung mast cells of guinea pig in anaphylactic shock. *Lab. Invest.* **37:** 1–17.

BORGERS, M., THORE, FL, VERHEYEN, A., and TER KEVRS, H. E. D. J. (1984). Localization of calcium in skeletal and cardiac muscle. *Histochm. J.* **16:** 295–309.

CAMPBELL, A. K. (1983). *Intracellular Calcium: Its Universal Role as Regulator.* Wiley, New York.

CHAN, S. Y., OCHS, S., and WORTH, R. M. (1980). The requirement for calcium ions and the effect of other ions in axoplasmic transport in mammalian nerve. *J. Physiol.* **301:** 477–504.

CHAN, S. Y., OCHS, S., and JERSILD, R. A. (1984). Localization of calcium in nerve fibers. *J. Neurobiol.* **15:** 89–105.

DUCE, I. R., and KEEN, P. (1978). Can neuronal smooth endoplasmic reticulum function as a calcium reservoir? *Neurosci.* **3:** 837–848.

FRIEDE, R. L., and BISCHAUSEN, R. (1980). The fine structure of stumps of transected nerve fibers in subserial sections. *J. Neurol. Sci.* **44:** 181–203.

HAPPEL, R. D., SMITH, K. P., BANIK, N. L., POWERS, J. M., HOGAN, E. L., and BALENTINE, J. E. (1981). Ca^{++} accumulation in experimental spinal cord trauma. *Brain Res.* **211:** 476–479.

HENKART, M. P., REESE, T. S., and BRINLEY, F. J. (1978). Endoplasmic reticulum sequesters calcium in the squid giant axon. *Science* **202:** 1300–1302.

HILLMAN, D. E., and LLINAS, N. (1974). Calcium containing electron dense structures in the axons of the squid giant synapse. *J. Cell. Biol.* **61:** 146–155.

KAMAKURA, K. L., ISHIURA, S., SUGITANO, H., and TOYOKURA, Y. (1981). Identification of calcium activated neutral protease in the rat peripheral nerve. *Biomed. Res.* **1:** 91–94.

KIRK, E. J. (1974). Impulsed in dorsal spinal nerve rootlets in cats and rabbits arising from dorsal root ganglia isolated from the periphery. *J. Comp. Neur.* **155:** 165–176.

LUBINSKA, L. (1977). Early course of Wallerian degeneration in myelinated fibers of the rat phrenic nerve. *Brain Res.* **130:** 47–63.

MALBOUISSON, A., GHABRIEL, M., and ALLT, G. (1984). The non-directional pattern of axonal changes in Wallerian degeneration: a computer aided morphometric analysis. *J. Anat.* **139:** 159–174.

MALBOUISSON, AL., GHABRIEL, M., and ALLT, G. (1985). Axonal degeneration in large and small nerve fibers-an electron-microscopic and morphometric study. *J. Neurol. Sci.* **67:** 307–327.

MALIK, M., FENKO, M., IQBAL, K., and WISNIEWSKI, H. (1983). Purification and characterization of two forms of calcium activated neutral protease from calf brain. *J. Biol. Chem.* **258:** 8955–8967.

OLSSON, Y. (1966). Studies of vascular permeability in peripheral nerves. I. Distribution of circulating fluorescent serum albumin in normal, crushed and sectioned rat sciatic nerve. *Acta Neuropath. Berl.* **7:** 1–5.

OSCHMAN, J. L., and WALL, B. J. (1972). Calcium binding to intestinal membranes. *J. Cell. Biol.* **55:** 58–73.

ROOMANS, G. M. (1980). Quantitative X-ray microanalysis of thin sections. In *X-Ray Microanalysis in Biology,* M. A. Hayat, Ed., University Park Press, Baltimore, MD, pp. 401–453.

SCHAMBER, F. W., WODKE, N. F., and MCCARTHY, J. J. (1977). Least squares fit with digital filter: the method and its application to EDS spectra. In *Eighth International Conference in X-Ray Optics Microanalysis,* D. R. Beamon, R. E. Ogilore, and D. B. Wittry, Eds., Pendell, Midland, MI, p. 98A.

SCHLAEPFER, W. W., and MICKO, S. (1978). Chemical and structural changes of neurofilaments in transected rat sciatic nerve. *J. Cell Biol.* **78:** 369–378.

SCHLAEPFER, W. W., and MICKO, S. (1979). Calcium dependent alterations of neurofilament proteins of rat peripheral nerve. *J. Neurochem.* **32:** 211–219.

SCHLAEPFER, W. W., LEE, C. L., LEE, V., and ZIMMERMAN, U. (1985). An immunoblot study of neurofilament degradation in situ and during calcium activate proteolysis. *J. Neurochem.* **44:** 502–509.

SCHLIWA, M. (1976). The role of divalent cations in the regulation of microtubule assembly. In vivo studies on microtubules in the heliozoan axopodium using the ionophore A23187. *J. Cell. Biol.* **59:** 456–470.

SUNDERLAND, S. (1978). *Nerves and Nerve Injuries.* Churchill Livingstone, London, pp. 82–107.

WADE, C. R., OHARA, P. T., and LIEBERMAN, A. R. (1980). Calcium localization in normal and degenerating myelinated nerve fibers of the CNS. *J. Anat.* **130:** 641–644.

WILLIAMS, P. L., and HALL, S. M. (1971). Prolonged in vivo observations of normal peripheral nerve fibers and their acute reactions to crush and deliberate trauma. *J. Anat.* **108:** 397–408.

YAWO, H., and KUNO, M. (1983). How a nerve fiber repairs its cut end: Involvement of phospholipase A_2. *Science* **222:** 1352–1353.

YAWO, H., and KUNO, M. (1985). Calcium dependence of membrane sealing at the cut end of the cockroach giant axon. *J. Neurosci.* **6:** 1626–1632.

YOUNG, W. YEN, V., and BLIGHT, A. (1982). Extracellular calcium ionic activity in experimental spinal cord contusion. *Brain Res.* **253:** 105–113.

ZIMMERMAN, V., and SCHLAEPFER, W. (1982). Characterization of brain calcium activated protease that degrades neurofilament proteins. *Biochem.* **21:** 3977–3983.